Published in final edited form as:
J Mol Cell Cardiol. 2014 January ; 66: 63–71. doi:10.1016/j.yjmcc.2013.10.021.

Cellular mechanisms of ventricular arrhythmias in a mouse model of Timothy syndrome (long QT syndrome 8)

Benjamin M. L. Drum, **Rose E. Dixon**, **Can Yuan**, **Edward P. Cheng**, and **Luis F. Santana**
Department of Physiology & Biophysics, University of Washington School of Medicine, Seattle, Washington 98195

Abstract

Ca^{2+} flux through L-type $Ca_V1.2$ channels shapes the waveform of the ventricular action potential (AP) and is essential for excitation-contraction (EC) coupling. Timothy syndrome (TS) is a disease caused by a gain-of-function mutation in the $Ca_V1.2$ channel ($Ca_V1.2$-TS) that decreases inactivation of the channel, which increases Ca^{2+} influx, prolongs APs, and causes lethal arrhythmias. Although many details of the $Ca_V1.2$-TS channels are known, the cellular mechanisms by which they induce arrhythmogenic changes in intracellular Ca^{2+} remain unclear. We found that expression of $Ca_V1.2$-TS channels increased sarcolemmal Ca^{2+} "leak" in resting TS ventricular myocytes. This resulted in higher diastolic $[Ca^{2+}]_i$ in TS ventricular myocytes compared to WT. Accordingly, TS myocytes had higher sarcoplasmic reticulum (SR) Ca^{2+} load and Ca^{2+} spark activity, larger amplitude $[Ca^{2+}]^i$ transients, and augmented frequency of Ca^{2+} waves. The large SR Ca^{2+} release in TS myocytes had a profound effect on the kinetics of $Ca_V1.2$ current in these cells, increasing the rate of inactivation to a high, persistent level. This limited the amount of influx during EC coupling in TS myocytes. The relationship between the level of expression of $Ca_V1.2$-TS channels and the probability of Ca^{2+} wave occurrence was non-linear, suggesting that even low levels of these channels were sufficient to induce maximal changes in $[Ca^{2+}]_i$. Depolarization of WT cardiomyocytes with a TS AP waveform increased, but did not equalize, $[Ca^{2+}]_i$ compared to depolarization of TS myocytes with the same waveform. We propose that $Ca_V1.2$-TS channels increase $[Ca^{2+}]$ in the cytosol and the SR, creating a Ca^{2+}overloaded state that increases the probability of arrhythmogenic spontaneous SR Ca^{2+} release.

Keywords

$Ca_V1.2$; Timothy syndrome; ventricular myocyte; excitation-contraction coupling; calcium wave

1. Introduction

The function of the heart is to pump blood. To achieve this function, the heart chambers must contract in a specific, electrically coordinated sequence. The cardiac electrical cycle starts with the firing of an action potential (AP) by sinoatrial node cells. This AP propagates

Contact information: Luis F. Santana, University of Washington, Box 357290, Seattle, WA 98195, Phone: 206-543-8681, santana@uw.edu.

Disclosures: none declared

via gap junctions to neighboring atrial myocytes and the atrio-ventricular node, eventually reaching the ventricles. Excitation-contraction (EC) coupling is the coordinated process by which this AP triggers cell contraction.

During the AP, depolarization of the sarcolemma briefly opens L-type $Ca_V1.2$ channels, thus allowing a small amount of Ca^{2+} to enter the cytosol [1–4]. The increased $[Ca^{2+}]_i$ in the cytosol activates ryanodine-sensitive Ca^{2+} channels in the sarcoplasmic reticulum (SR) via the mechanism called "Ca^{2+}-induced Ca^{2+} release" (CICR) [5]. This results in the production of a "Ca^{2+} spark"[6]. Synchronous activation of thousands of Ca^{2+} sparks throughout the myocytes causes a cell-wide increase in $[Ca^{2+}]_i$ that triggers contraction. Closure of $Ca_V1.2$ channels, due to inactivation and membrane repolarization, terminates both Ca^{2+} influx and release. Re-sequestration of Ca^{2+} into the SR by the Ca^{2+} ATPase and Ca^{2+} extrusion by the sarcolemmal Na^+/Ca^{2+} exchanger (NCX) restores $[Ca^{2+}]_i$ to diastolic levels.

This process of Ca^{2+} release and recovery is critical for the physiological heartbeat. Disruption of the cycle via prolongation of the AP can lead to an inability of the cell to return to diastolic levels before the next systole, thus creating spontaneous Ca^{2+} release and fatal arrhythmia. Long QT syndrome is one set of disorders in which ventricular repolarization is prolonged. Timothy syndrome (TS), also known as long QT syndrome 8, is a rare childhood disorder caused by a single amino acid substitution (G406R) in exon 8 of $Ca_V1.2$, creating a mutant channel ($Ca_V1.2$-TS) [7]. It is an autosomal dominant, multisystem disorder, leading to congenital heart disease, syndactyly, immunodeficiency, cognitive abnormalities, and autistic spectrum defects. TS patients commonly suffer sudden cardiac death as a result of lethal cardiac arrhythmias characterized by a long QT interval [7].

In the sarcolemma, $Ca_V1.2$ channels can exist in 3 gating modes: 0, 1, and 2. $Ca_V1.2$ channels in mode 0 are closed [8]. In mode 1, $Ca_V1.2$ channels have a low open probability (P_o) and undergo brief openings (<1 ms). In contrast, $Ca_V1.2$ channels in mode 2 have a high P_o and relatively long open times (>10 ms). $Ca_V1.2$ channels in this mode of operation allow relatively large amounts of Ca^{2+} to enter the cell [9, 10]. $Ca_V1.2$-TS channels exhibit increased "mode 2" gating, and undergo a slower voltage-dependent inactivation (VDI). Together, these properties contribute to a longer mean open time of these channels compared to WT channels [11, 12].

We generated transgenic mice expressing variable levels of $Ca_V1.2$-TS solely in cardiac myocytes (TS mice) [13]. TS mice have a long QT interval and increased arrhythmia frequency despite having similar resting and exercise heart rates [13]. Two studies have investigated the effects of $Ca_V1.2$-TS channels on $[Ca^{2+}]_i$ in cultured inducible pluripotent stem cell-derived cardiomyocytes and rat ventricular myocytes [14, 15]. Although important, these studies focused on Ca^{2+} current changes, leaving some biophysical aspects of EC coupling unexplored, which are difficult to study in cultured adult or immature myocytes due to absence or loss of transverse tubules. Thus, the mechanisms by which $Ca_V1.2$-TS causes arrhythmogenic changes in $[Ca^{2+}]_i$ remain unclear. In the present study, we found that even a low level of expression of $Ca_V1.2$-TS is sufficient to dramatically alter $[Ca^{2+}]_i$ in ventricular myocytes. $Ca_V1.2$-TS channels increased resting $[Ca^{2+}]_i$, SR load, Ca^{2+} spark frequency and amplitude, AP-evoked $[Ca^{2+}]_i$ transients, and probability of Ca^{2+} waves, providing evidence that $[Ca^{2+}]$ increases in both the cytosol and SR. We propose that $Ca_V1.2$-TS channels create a Ca^{2+} overloaded state that increases the probability of arrhythmogenic events due to spontaneous SR Ca^{2+} release.

2. Material and methods

2.1. Isolation of ventricular myocytes

Mice (TS and WT controls) were euthanized with a lethal dose of sodium pentobarbital administered intraperitoneally as approved by the University of Washington Institutional Animal Care and Use Committee. Ventricular myocytes were isolated using a Langendorff perfusion apparatus as previously described [16, 17]. The isolated ventricular myocytes were kept at room temperature (22–25 °C) in Tyrode's solution containing (mM): 140 NaCl, 5 KCl, 10 HEPES, 10 glucose, 2 $CaCl_2$, and 1 $MgCl_2$; pH 7.4 with NaOH, and used 0.5–8 hours after isolation.

2.2 Additional experimental methods

Please see Appendix A for online data supplement with additional experimental methods.

2.3. Statistics

Data are presented as mean ± standard error of the mean (S.E.M.). Two-sample comparisons were made using a Student's *t* test (* $P < 0.05$, ** $0.001 < P \leq 0.01$, *** $P \leq 0.001$).

3. Results

3.1. Higher resting sarcolemmal Ca^{2+} leak and $[Ca^{2+}]_i$ transients in TS compared to WT ventricular myocytes

We have three TS mouse lines. Real time PCR was used to quantify $Ca_V1.2$-TS transcript expression in these lines (Figure S1*A*). Data were normalized to β-actin mRNA levels because it was expressed to a similar extent in WT and TS lines. Using this analysis, we found increasing levels of $Ca_V1.2$-TS channels in our 3 TS lines with line 1 expressing the lowest and 3 the highest mRNA ($n = 3$ mice per group; $P < 0.01$) (Figure S1*A*). We also quantified relative protein expression of $Ca_V1.2$-TS compared to $Ca_V1.2$-WT in these lines and found that line 1 expression was 0.20 ± 0.04, line 2 was 0.40 ± 0.3, and line 3 expression was 1.54 ± 0.68 ($n = 4$ mice per group; $P < 0.05$) (Figure S1*B*). The relationship between $Ca_V1.2$-TS mRNA and protein was linear, suggesting that higher mRNA translated into higher $Ca_V1.2$-TS protein expression in ventricular myocytes (Figure S1*C*). Unless specified, TS line 1 was used in the experiments described below because the expression level of this channel is similar in humans with TS [12].

To examine $[Ca^{2+}]_i$ in WT and TS myocytes, cells were loaded with the fluorescent Ca^{2+} indicators Asante Ca^{2+} Red (ACaR) or Fluo-4 AM and imaged using a confocal microscope. ACaR is a ratiometric Ca^{2+} indicator that can be excited with 488 nm light. The emission spectrum of the Ca^{2+}-free and -bound forms of ACaR peak at 525 and 650 nm, respectively. The ratio ACaR fluorescence at 650 and 525 nm increases ≈35-fold when $[Ca^{2+}]$ goes from Ca^{2+}-free to saturating levels. Like ACaR, the single wavelength indicator Fluo-4 was excited with 488 nm light. Fluo-4 emission was measured at 525 nm. Fluo-4 undergoes much larger changes in fluorescence than ACaR in response to changes in Ca^{2+}, increasing ≈255-fold when $[Ca^{2+}]$ is elevated from Ca^{2+}-free to saturating levels.

The relationship between the fluorescence intensities of ACaR or Fluo-4 and $[Ca^{2+}]$ is non-linear. Thus, ACaR and Fluo-4 fluorescence values were converted to concentration (nM) units as described by Grynkiewicz *et al.* [18] and Maravall *et al.* [19], respectively. The rationale for using these two indicators in the initial set of experiments was manifold. Although the ratiometric ACaR has a lower dynamic range than Fluo-4, it has the advantage that its calibration is not affected by dye concentration or photo-bleaching rates. Fluo-4's large dynamic range makes it a better choice for the detection of small $[Ca^{2+}]_i$ levels than

ACaR in TS and WT myocytes. However, because Fluo-4 is a single wavelength indicator, calibrating it assumes no change in laser intensity, photomultiplier gain, pinhole size, and indicator concentration during the experiment. By comparing the $[Ca^{2+}]_i$ values obtained using ACaR or Fluo-4, we tested the assumption that these parameters did not change during Fluo-4 experimentation, which would validate the calibration of this indicator.

We recorded action potential (AP)-evoked $[Ca^{2+}]_i$ transients in TS and WT myocytes. APs were evoked via field stimulation at a frequency of 1 Hz. Figure 1*A–B* shows representative AP-evoked $[Ca^{2+}]_i$ transients in WT and TS cells under steady-state conditions. The amplitude of the global $[Ca^{2+}]_i$ transient was larger in TS than in WT cells whether it was measured using ACaR (WT = 560 ± 46 nM, n = 8 vs. TS = 1003 ± 151 nM, n = 10; $P < 0.05$) or Fluo-4 (WT = 600 ± 40 nM, n = 49 vs. TS = 1000 ± 62 nM, n = 56; $P < 0.001$). Diastolic $[Ca^{2+}]_i$ — defined as the $[Ca^{2+}]_i$ measured at the end of the 1 s interval between APs — was also higher in TS than in WT cells in ACaR (WT = 152 ± 17 nM, n = 8 vs. TS = 237 ± 15 nM, n = 10; $P < 0.01$) and Fluo-4-loaded cells (WT = 158 ± 8 nM, n = 9 vs. TS = 215 ± 7 nM, n = 10; $P < 0.001$). $[Ca^{2+}]_i$ in non-stimulated, resting myocytes (measured at least 2 seconds after the cessation of stimulation) was also higher in TS (ACaR = 222 ± 13 nM, n = 10 vs. Fluo-4 = 215 ± 15 nM, n = 10) than in WT myocytes (ACaR = 144 ± 12 nM, n = 8 vs. Fluo-4 = 150 ± 6 nM, n = 7; ACaR $P < 0.001$, Fluo-4 $P < 0.01$) (Figure 1*C*).

We tested the hypothesis that higher "Ca^{2+} leak" through sarcolemmal $Ca_V1.2$ channels contributes to higher resting $[Ca^{2+}]_i$ in TS than in WT myocytes (Figure 1*D*). To test this hypothesis, we recorded $[Ca^{2+}]_i$ in resting TS and WT myocytes before and after the application of a 0 Na^+/0 Ca^{2+} external solution in the presence or absence of the $Ca_V1.2$ channel blocker nifedipine (10 μM). All solutions in these experiments contained the SERCA pump inhibitor thapsigargin (1 μM) to eliminate SR Ca^{2+} release. As shown in the representative traces in Figure 1*D*, application of the 0 Na^+/0 Ca^{2+} external solution decreased $[Ca^{2+}]_i$ in TS and WT myocytes, presumably due to the termination of Ca^{2+} leak via Na^+/Ca^{2+} exchanger and Ca^{2+}-permeable channels and extrusion via the sarcolemmal Ca^{2+} pump. In the WT myocyte, return to the Ca^{2+} containing extracellular solution increased resting $[Ca^{2+}]_i$ to control levels (150 ± 4 nM, n =6) even in the presence of nifedipine (153 ± 4 nM, n = 6, $P > 0.05$). This suggests that Ca^{2+} flux via $Ca_V1.2$ channels does not contribute to resting $[Ca^{2+}]_i$ in WT myocytes. However, in TS myocytes, $[Ca^{2+}]_i$ increased only to 160 ± 4 nM upon return to control conditions in the presence of nifedipine compared to 207 ± 13 nM without nifedipine ($P < 0.05$).

We differentiated these records to determine the rate of change in resting $[Ca^{2+}]_i$ during the switch from the 0 Na^+/0 Ca^{2+} to the 2 mM external Ca^{2+} solution. The maximum $d[Ca^{2+}]_i/dt$ was 0.0010 ± 0.0001 nM/ms and 0.004 ± 0.001 nM/ms in WT and TS myocytes ($P < 0.05$), respectively. By contrast, the maximum $d[Ca^{2+}]_i/dt$ of the AP-evoked $[Ca^{2+}]_i$ transients in the presence of 1 μM thapsigargin was 2.5 ± 0.1 nM/ms (n = 8 WT cells). Thus, while the maximum rate of Ca^{2+} influx at rest is faster in TS than in WT myocytes, it is about three orders of magnitude slower than the rate of Ca^{2+} influx into a ventricular myocyte during EC coupling.

Collectively, these data suggest that TS myocytes have a higher resting, diastolic, and systolic $[Ca^{2+}]_i$ than WT myocytes. Although Ca^{2+} influx through $Ca_V1.2$ channels does not contribute to resting $[Ca^{2+}]_i$ in WT cells, expression of $Ca_V1.2$-TS channels results in higher resting sarcolemmal leak and consequently higher $[Ca^{2+}]_i$ in TS than in WT cells. Furthermore, our data indicate that ACaR and Fluo-4 report similar $[Ca^{2+}]_i$ in ventricular myocytes, suggesting that laser intensity, photomultiplier gain, pinhole size, and Fluo-4 concentration did not change under our experimental conditions. Thus, calibration of Fluo-4

using the Maravall *et al.* [19] method is valid. Based on this, and the higher dynamic range of Fluo-4, this indicator was used in the experiments presented below.

3.2. TS myocytes have a higher frequency of Ca^{2+} sparks and waves than WT myocytes

We investigated the mechanisms underlying higher $[Ca^{2+}]_i$ transients in TS myocytes. Experiments tested the hypothesis that RyR activity is higher in TS myocytes than in WT myocytes. A testable prediction of this hypothesis is that spontaneous Ca^{2+} spark activity is higher in TS myocytes than in WT myocytes.

Figure 2*A* shows representative confocal line-scan images of Ca^{2+} sparks in quiescent/resting WT and TS cells. Consistent with our hypothesis, we found that spontaneous Ca^{2+} spark frequency was ≈3.5-fold higher in TS (3.8 ± 0.6 sparks/100 μm/s, n = 11 cells) than in WT cells (1.1 ± 0.2 sparks/100 μm/s, n = 15 cells; $P < 0.01$) (Figure 2*B*). Ca^{2+} sparks in TS cells also had larger amplitude (401 ± 3 nM, n = 1602 vs. 297 ± 2 nM, n = 1782, $P < 0.01$) (Figure 2*C*) and full width at half-maximal amplitude (4.0 ± 0.1 ms, n = 1602 vs. 3.6 ± 0.1 ms, n = 1782; $P < 0.05$) (Figure 2*D*) compared to WT cells. Ca^{2+} spark duration, however, was similar in these cells (WT = 45 ± 1 ms, n = 1782 vs. TS = 44 ± 1 ms, n = 1602; $P > 0.05$) (Figure 2*E*).

If higher Ca^{2+} channel activity is sufficient to increase resting $[Ca^{2+}]_i$ and thus induce higher Ca^{2+} spark activity in TS than in WT ventricular myocytes, exposing WT cells to a $Ca_V1.2$ channel opener should increase Ca^{2+} spark frequency in these cells to a level similar to that of TS cells. Figure 2*F* shows a representative line-scan image of a quiescent WT cell exposed to 1 μM FPL 64176, a drug known to increase the open probability of $Ca_V1.2$ channels. Consistent with our hypothesis, FPL 64176 increased resting $[Ca^{2+}]_i$ (from 150 ± 16 to 209 ± 26 nM) and Ca^{2+} spark frequency in WT cells to a level similar to the one observed in TS cells (3.0 ± 0.4 sparks/100 μm/s, n = 10 cells; $P < 0.05$) (Figure 2*H*). Application of 1 μM FPL 64176 to TS cells invariably induced Ca^{2+} waves and cell death. It is important to note, that the effects of FPL 64176 on WT and TS myocytes were not rapid. Rather, the effects of FPL 64176 on Ca^{2+} spark (or waves) activity were seen approximately 3 minutes after exposure to the drug, during which time the cell was not stimulated. Similarly, short-term application (i.e., <20 s) of nifedipine (10 μM) did not affect Ca^{2+} spark frequency in WT and TS cells ($P > 0.05$) (Figure 2*G–H*). This suggests that spontaneous Ca^{2+} sparks are not directly activated or produced by the opening of $Ca_V1.2$ channels in TS or WT myocytes.

Having determined that TS myocytes have a higher propensity to undergo spontaneous SR Ca^{2+} release than WT myocytes, we performed a quantitative analysis of arrhythmogenic spontaneous Ca^{2+} waves in these cells. Figure 3*A* shows representative line-scan images of a large, non-propagated Ca^{2+} spark in a WT myocyte and a Ca^{2+} wave in a TS cell. Indeed, we found that while in WT cells Ca^{2+} waves are rare (1 wave per 308 ± 166 s, n = 25), the frequency of Ca^{2+} waves is dramatically higher in TS myocytes (1 wave per 49.4 ± 16.8 s, n = 37; $P < 0.05$) (Figure 3*B*). This relationship is maintained even upon application of 100 nM of the β adrenergic receptor agonist isoproterenol (WT, 1 wave per 31.7 ± 9.0 s, n = 17 vs. TS, 17.1 ± 2.7 s, n = 22; $P < 0.05$) (Figure 3*C*). Analysis of the Ca^{2+} waves suggested that they propagate at a faster rate in TS (87.4 ± 1.7 μm/s, n = 147) than in WT cells (77.7 ± 2.6 μm/s, n = 25; $P < 0.05$) (Figure 3*D*).

We extended this Ca^{2+} analysis to the other two $Ca_V1.2$-TS mouse lines to investigate the relationship between $Ca_V1.2$-TS expression and arrhythmogenic Ca^{2+} wave activity in ventricular myocytes. Interestingly, although only 5 ± 3% of the WT myocytes (n = 12) had spontaneous Ca^{2+} waves, 50 ± 3 (n = 16), 65 ± 8 (n = 19), and 70 ± 10% (n = 22) of the

myocytes isolated from TS mice lines 1–3 had Ca^{2+} waves (Figure 3*E*). This suggests a nonlinear relationship between TS expression and aberrant Ca^{2+} wave activity in a cell.

3.3. Higher SR Ca^{2+} load in TS than in WT ventricular myocytes

A potential mechanism for a higher frequency of spontaneous Ca^{2+} sparks, Ca^{2+} waves, and larger AP–evoked $[Ca^{2+}]_i$ transients is an elevation in the SR Ca^{2+} load. Thus, we tested the hypothesis that SR Ca^{2+} content was higher in TS than in WT myocytes. We used a picospritzer to rapidly apply a Na^+- and Ca^{2+}-free saline solution containing 20 mM caffeine to both paced and quiescent/resting WT and TS cells. Figure 4*A* shows caffeine-induced $[Ca^{2+}]_i$ transients from representative resting TS and WT myocytes. Under these experimental conditions, the amplitude of the caffeine induced $[Ca^{2+}]_i$ transient was ≈1.5-fold higher in TS (1666 ± 109 nM, $n = 11$) compared to WT cells (1090 ± 66 nM, $n = 17$; $P < 0.01$) (Figure 4*C*), suggesting that TS myocytes have a higher SR Ca^{2+} load than WT myocytes.

Figure 4*B* shows caffeine-induced $[Ca^{2+}]_i$ transients from representative TS and WT myocytes which had been paced at 1 Hz until reaching steady-state. At this frequency, the amplitude of the $[Ca^{2+}]_i$ transient of TS and WT myocytes reached steady state after 7 APs. On average, the amplitude of the caffeine-induced $[Ca^{2+}]_i$ transient in paced cells was ≈1.4-fold higher in TS (1207 ± 66 nM, $n = 60$) compared to WT cells (828 ± 59 nM, $n = 49$; $P < 0.01$) (Figure 4*C*).

3.4. The large SR Ca^{2+} release during EC coupling in TS cells increases the rate of inactivation of I_{Ca} and hence limits Ca^{2+} influx during membrane depolarization into these cells

In the heart, the Ca^{2+} current (I_{Ca}) triggers SR Ca^{2+} release during EC coupling. Membrane depolarization opens $Ca_V1.2$ channels, but these channels inactivate due to Ca^{2+}-dependent and voltage-dependent mechanisms [20]. SR Ca^{2+} release is a major contributor to Ca^{2+}-dependent inactivation of I_{Ca} [21]. Although $Ca_V1.2$-TS currents inactivate at a slower rate than WT channels, the effects of SR Ca^{2+} release on these currents are unknown.

Figure 5*A* shows representative I_{Ca} records from TS and WT myocytes dialyzed with an intracellular solution containing 10 mM of the Ca^{2+} chelator EGTA to maintain low global $[Ca^{2+}]_i$ and eliminate SR Ca^{2+} release. Peak I_{Ca} at 0 mV was −1154 ± 202 pA in WT ($n = 5$) and 1734 ± 541 pA in TS cells ($n = 6$). However, because TS cells (214 ± 25 pF) had a higher capacitance than WT cells (171 ± 25 pF), I_{Ca} density (i.e., pA/pF) was similar in these cells (WT = −6.9 ± 1.1 pA/pF vs. TS = −7.7 ± 1.8 pA/pF; $P > 0.05$). We fitted the decaying phase of these currents with the sum of two exponential functions. The time constants of the fast (τ_{fast}; WT = 26 ± 4 ms vs. TS = 38 ± 4 ms; $P < 0.05$) and slow component (τ_{slow}; WT = 84 ± 7 ms vs. TS = 136 ± 13 ms; $P < 0.01$) were larger in TS than in WT cells. Accordingly, the total charge associated with the I_{Ca} recorded from EGTA-dialyzed cells (determined by integrating these currents) was −688 ± 208 fC/pF in TS ($n = 6$) compared to −455 ± 98 fC/pF in WT cells ($n = 5$) (Figure 5*A*).

Figure 5*C* shows line-scan images, I_{Ca} densities, and the time course of the spatially-averaged $[Ca^{2+}]_i$ of TS and WT cells depolarized to the test potential of 0 mV. EGTA was absent from the patch pipette solution to ensure normal SR Ca^{2+} release during membrane depolarization. To achieve steady-state SR Ca^{2+} load, 10 pre-conditioning pulses (100 ms duration) from −80 to 0 mV (1 Hz) were applied just prior to the test pulse. Control experiments showed that TS myocytes (amplitude of the caffeine-induced transient = 1224 ± 74 nM) had a higher SR Ca^{2+} load than WT cells (amplitude of the caffeine-induced transient = 828 ± 59 nM) when depolarized with a similar waveform ($P < 0.05$). Test pulses

began with a slow ramping depolarization (0.08 mV/ms) from −80 mV to −50 mV, where the cell was held for 50 ms to inactivate Na^+ channels. In addition, to ensure no contaminating Na^+ channel currents, 10 μM tetrodotoxin was added to the perfusion solution. Cells were then depolarized for 200 ms from this interim holding potential to voltages ranging from −40 to +60 mV.

Although, on average, peak I_{Ca} density was similar in WT and TS cells, the $[Ca^{2+}]_i$ transients these currents evoked were larger in TS (n = 7) than in WT myocytes (n = 7) at all voltages examined (Figure 5*D*; P < 0.05). Consequently, EC coupling gain, defined here as the maximum change in $[Ca^{2+}]_i$ divided by the peak I_{Ca} density at a given voltage, tended to be higher in TS than in WT cells over a broad range of voltages (Figure 5*E*).

Interestingly, with SR Ca^{2+} release enabled, I_{Ca} inactivated at a faster rate in TS than in WT cells. This was largely due to a faster first component in TS (τ_{fast} = 6 ± 1 ms, n = 6) than in WT cells (τ_{fast} = 14 ± 2 ms, n = 5; P < 0.05), as τ_{slow} was similar in these cells (WT = 61 ± 17 ms, n = 5 vs. TS = 60 ± 11 ms, n = 6; P > 0.05). However, because TS cells had a larger noninactivating component, total Ca^{2+} flux during the 200 ms pulse was ≈1.5-fold higher in TS cells (−389 ± 60 fC/pF, n = 3) than WT cells (−256 ± 8 fC/pF, n = 5; P < 0.05) (Figure 5*B*).

Taken together, the data in Figure 5 suggest that SR Ca^{2+} release and EC coupling gain are larger in TS than in WT myocytes. SR Ca^{2+} release has a profound impact on the kinetics of I_{Ca} in TS cells. In the absence of EC coupling I_{Ca} inactivates at a slower rate in TS than in WT myocytes. However, with SR Ca^{2+} release, I_{Ca} inactivates faster, but to a sustained current level in TS cells.

3.5. Differences in AP waveform amplify differences in Ca^{2+} influx between TS and WT myocytes

Although the use of square voltage pulses to evoke I_{Ca} is convenient for technical and analytical purposes, they do not provide information on Ca^{2+} influx during the physiological AP. We used the AP clamp technique to test the hypothesis that Ca^{2+} influx is larger in TS than in WT myocytes during the AP. Myocytes were depolarized with a previously recorded WT or TS AP (Figure 6*A*). Figure 6*B–C* shows averaged AP-evoked Ca^{2+} current traces from WT and TS myocytes in the absence or presence of 10 μM nifedipine. In WT cells, the TS AP evoked currents with a larger peak (−4.9 ± 0.5 pA/pF, n = 9) and integral (−37.0 ± 4.9 fC/pF, n = 9) than the WT AP (peak, −1.6 ± 0.5 pA/pF, n = 11; integral, −6.2 ± 1.7 fC/pF, n = 11; P < 0.001) (Figure 6*D–E*). Similarly, in TS cells, the TS AP evoked currents with a larger peak (−7.0 ± 0.4 pA/pF, n = 11) and integral (−55.2 ± 2.9 fC/pF, n = 11) than the WT AP (peak, −1.1 ± 0.2 pA/pF, n = 11; integral, −5.0 ± 1.2 fC/pF, n = 11; P < 0.001). Interestingly, applying the TS AP evoked a greater response from TS myocytes (−55.2 ± 2.9 fC/pF, n = 11) than WT myocytes (−37.0 ± 4.9 fC/pF, n = 9; P < 0.01) (Figure *6B–E*). Strong reduction of these AP-evoked currents with 10 μM nifedipine suggests that these currents are produced by Ca^{2+} influx via $Ca_V1.2$ channels (Figure 6*B–E*). Importantly, these data suggest that both AP waveform and $Ca_V1.2$-TS gating properties contribute to the increase in I^{Ca} seen in TS.

3.6. Differences in AP waveform contribute to differences in EC coupling between WT and TS cells

Next, we tested the hypothesis that differences in the AP waveform between WT and TS cells contribute to differences in $[Ca^{2+}]_i$ between these cells. A testable prediction of this hypothesis is that if differences in $[Ca^{2+}]_i$ between WT and TS cells were due exclusively to differences in AP waveform, then $[Ca^{2+}]_i$ transients of WT cells stimulated with TS APs

should resemble TS cells and vice versa. Thus, we recorded $[Ca^{2+}]_i$ transients while using a AP clamp to again apply WT or TS AP waveforms.

Figure 7*A–B* shows a set of confocal line-scan images and $[Ca^{2+}]_i$ transients from representative WT and TS cells depolarized with WT and TS APs. As expected, WT cells stimulated with a WT AP had smaller $[Ca^{2+}]_i$ transients (717 ± 35 nM, $n = 13$) compared to TS cells stimulated with a TS AP (1144 ± 35 nM, $n = 13$; $P < 0.01$). In addition, we found that WT cells stimulated with TS APs had larger $[Ca^{2+}]_i$ transients than when stimulated with WT APs, and TS cells stimulated with WT APs had smaller $[Ca^{2+}]_i$ transients than when stimulated with TS APs. Interestingly, however, the amplitudes of these transients were not recapitulations of WT or TS cells. Rather, the $[Ca^{2+}]_i$ transient of WT cells depolarized with a WT AP (717 ± 35 nM, $n = 13$) was smaller in amplitude compared to the $[Ca^{2+}]_i$ transients of TS cells depolarized with a WT AP (878 ± 29 nM, $n = 11$; $P < 0.05$). Similarly, the $[Ca^{2+}]_i$ transient of TS cells depolarized with a TS AP (1144 ± 35 nM, $n = 13$) was larger in amplitude compared to the $[Ca^{2+}]_i$ transients of WT cells depolarized with a TS AP (831 ± 33 nM, $n = 13$; $P < 0.05$) (Figure *7C*). These data indicate that differences in AP waveform contribute to, but do not sufficiently account for the differences in $[Ca^{2+}]_i$ transients observed between WT and TS cells.

4. Discussion

We performed a detailed biophysical analysis of the functional consequences of $Ca_V1.2$-TS channel expression on EC coupling in adult ventricular myocytes. On the basis of these data, we propose a mechanistic model for how $Ca_V1.2$-TS channels alter $[Ca^{2+}]_i$ and EC coupling in ventricular myocytes. Our data indicate that expression of $Ca_V1.2$-TS increases resting and AP-evoked Ca^{2+} influx into ventricular myocytes. This is associated with an increase in diastolic $[Ca^{2+}]_i$ and SR Ca^{2+} load that likely augments the frequency and amplitude of spontaneous Ca^{2+} sparks in TS cells. Accordingly, AP-evoked $[Ca^{2+}]_i$ transients were larger in TS than in WT myocytes. Furthermore, we found that there is a non-linear relationship between the expression of $Ca_V1.2$-TS channel and Ca^{2+} wave frequency, suggesting that relatively low levels of $Ca_V1.2$-TS expression induces a disproportionally large increase in the probability of arrhythmogenic SR Ca^{2+} release events in ventricular myocytes.

The mouse model of TS we generated expresses WT $Ca_V1.2$ channels and mutant $Ca_V1.2$ channels with the glycine at position 406 substituted by an arginine, which promotes mode 2 gating of $Ca_V1.2$-TS channels [9]. Recent studies suggest two potential mechanisms by which the G406R substitution alters $Ca_V1.2$-TS gating. Erxleben *et al.* [9] suggested that this G406R mutation creates a new phosphorylation site for the CaMKII. In their experiments in HEK293 cells, CaMKII was critical for mode 2 gating by $Ca_V1.2$-TS channels. Thiel *et al.* [14] reached a similar conclusion using cultured ventricular myocytes. Others, however, suggest that phosphorylation by CaMKII may not be necessary for $Ca_V1.2$-TS channels to have a slower rate of inactivation than WT channels [13, 22].

Cheng *et al.* [13] proposed an alternative model for $Ca_V1.2$-TS channel dysfunction during Timothy syndrome. In this model, the anchoring protein AKAP150 and $Ca_V1.2$-TS form a complex that is necessary for aberrant $Ca_V1.2$-TS channel gating and arrhythmias. $Ca_V1.2$-TS channels likely interact with AKAP150 via leucine zipper motifs in the C-terminals of these proteins [23]. AKAP150 functions like an allosteric modulator of $Ca_V1.2$-TS channels, increasing $Ca_V1.2$-TS currents by stabilizing the open conformation (i.e., mode 2 gating) and increasing the probability of coupled gating between $Ca_V1.2$-TS channels [13, 16, 24]. The longer openings of $Ca_V1.2$-TS channels are due, at least in part, to decreased voltage-dependent inactivation of these channels [11]. This leads to increased Ca^{2+} influx, AP prolongation, cardiac hypertrophy, and arrhythmias. Coupled gating of $Ca_V1.2$-TS channels

presumably occurs because AKAP150 promotes physical interactions of adjacent channels via their C-tails [23–25]. Thus, a combination of frequent, longer, and coupled openings of $Ca_V1.2$-TS channels increases Ca^{2+} influx even with shorter APs. Furthermore, although increasing K^+ channel conductance is likely to decrease Ca^{2+} influx, it may not be sufficient to eliminate the pathology.

Our data suggest that the impact of $Ca_V1.2$-TS channels on myocyte $[Ca^{2+}]_i$ extends beyond the AP. Indeed, we found that resting and diastolic $[Ca^{2+}]_i$ was higher in TS than in WT myocytes. In quiescent myocytes, $[Ca^{2+}]_i$ is largely determined by the balance between Ca^{2+} extrusion and influx through the sarcolemma. The two primary pathways of Ca^{2+} influx are $Ca_V1.2$ channels and the Na^+/Ca^{2+} exchanger (NCX) in its "reverse mode" of operation. Ca^{2+} is extruded by the NCX in its forward mode and, to a much lower extent, by the sarcolemmal Ca^{2+} pump [26, 27]. Because at the diastolic potential of ventricular myocytes (−80 mV) the open probability of WT $Ca_V1.2$ channels is very low, Ca^{2+} influx through these channels is also minimal. Consistent with this, we found that application of nifedipine does not alter resting $[Ca^{2+}]_i$ in WT ventricular myocytes. However, $Ca_V1.2$-TS channels have a higher level of activity than WT channels even at diastolic membrane potentials [13, 24]. Accordingly, nifedipine-sensitive Ca^{2+} influx — presumably via $Ca_V1.2$-TS channels — contributes to higher resting $[Ca^{2+}]_i$ in TS than in WT myocytes. Thus, while in WT myocytes resting $[Ca^{2+}]_i$ is largely determined by the NCX and to a lesser extent the sarcolemmal Ca^{2+} pump, in TS cells $Ca_V1.2$-TS channels represent a new Ca^{2+} "leak" pathway at rest. Yet, our analysis indicate that this Ca^{2+} leak is likely due to a relatively low number of persistently open $Ca_V1.2$-TS channels open at rest, as the rate of Ca^{2+} influx at these potentials is orders of magnitude lower than during the AP.

Our results show that the TS phenotype not only increases cytosolic $[Ca^{2+}]$ directly via increased flux through TS channels, it also increases the SR load and causes the SR to be more leaky. As noted above, CaMKII signaling has been implicated in SR leak, has been found to be activated in TS [14, 28, 29]. Bradshaw *et al.* [30] found that CaMKII activation is relatively insensitive to resting $[Ca^{2+}]$. Indeed, they found that a $[Ca^{2+}]_i \approx 3.2$ μM is needed to activate 50% CaMKII *in vitro*. Consistent with this, the Bers group [31, 32] found that the majority of CaMKII activation in ventricular myocytes was found in areas of local high $[Ca^{2+}]_i$, such as the dyadic cleft. Thus, we speculate that these high Ca^{2+} areas would be both more abundant and richer in Ca^{2+} in TS due to increased Ca^{2+} sparklets [13, 24], Ca^{2+} spark activity, higher Ca^{2+} transients, and Ca^{2+} wave activity. CaMKII activation in these areas could further augment SR leak and increase mode 2 gating of TS and WT channels in TS cells, creating a feed-forward mechanism that could increase the probability of arrhythmogenic changes in Ca^{2+} signaling. Furthermore, it is intriguing to speculate that the seemingly contradictory reports [13, 22] on the role of CaMKII on $Ca_V1.2$-TS channel function may reflect differences in local Ca^{2+} signaling and thus the activity of this kinase. Future experiments should examine this issue in detail.

Our data suggest that SR Ca^{2+} release had a profound impact on the kinetics of I_{Ca} in TS cells, greatly accelerating the rate of inactivation of this current. This is important because SR Ca^{2+} release increased CDI, limiting Ca^{2+} influx into TS myocytes. Because CDI is unaffected in TS channels [11], the faster rate of inactivation is likely due to the faster CDI of WT and TS $Ca_V1.2$ channels in TS cells. Note, however, that while I^{Ca} inactivates at a much lower rate in TS than in WT in the absence of EC coupling, with SR Ca^{2+} release enabled, TS I_{Ca} inactivates faster than WT cells, albeit to a higher sustained level. We propose that SR Ca^{2+} release forms part of a negative feedback mechanism that decreases Ca^{2+} influx in TS cells by increasing CDI of WT and TS $Ca_V1.2$ channels.

An important observation in this study is that the relationship between the level of expression of $Ca_V1.2$-TS channels and the probability of Ca^{2+} wave occurrence was non-linear. This suggests that even low levels of these channels are sufficient to induce maximal changes in $[Ca^{2+}]_i$. A potential mechanism by which a relatively small number of $Ca_V1.2$ channels could have a disproportionally large effect on $[Ca^{2+}]_i$ was proposed by Dixon *et al.* [33], who found that $Ca_V1.2$-TS channels can physically interact with WT $Ca_V1.2$ channels. When they do, WT channel activity increases to a level similar to that of TS channels. In this context, even a small level of expression of functional TS channels could have a disproportionally large effect on Ca^{2+} influx by making adjoined WT channels function like TS channels. Fusion of channels increases I_{Ca} by increasing the open probability of adjoining channels. It is intriguing to speculate that in heterozygous humans expressing G406R $Ca_V1.2$-TS channels, where these channels account for only ~12% of $Ca_V1.2$ channels, coupling of WT and TS channels amplifies Ca^{2+} influx and thus increases the probability of SR Ca^{2+} overload and arrhythmias [12].

Furthermore, the relationship between $[Ca^{2+}]_i$ and Ca^{2+} overload has been well characterized and shown to be highly nonlinear. A two-fold increase in diastolic $[Ca^{2+}]_i$ could lead to up to an 84-fold increase in pathological Ca^{2+} activity such as Ca^{2+} waves [34]. This non-linear relationship between $Ca_V1.2$-TS expression and Ca^{2+} waves arises from an increase in basal $[Ca^{2+}]_i$, SR Ca^{2+} content, and Ca^{2+} spark properties such as frequency and amplitude as well as the non-linear combinatorics of these properties' influence (e.g., RyR Ca^{2+} sensitivity) on Ca^{2+} wave development. In line with these results, we have found that even low levels of TS expression lead to a ≈1.4-fold increase in diastolic $[Ca^{2+}]_i$, a ≈3-fold increase in Ca^{2+} spark frequency, and a ≈10-fold increase in Ca^{2+} wave frequency. Furthermore, it is important to note that potential changes in the electrical properties of the TS cells (e.g., decreased inward rectifying K^+ currents) could conspire with higher $[Ca^{2+}]_i$ to increase the probability of arrhythmogenic voltage fluctuations in these cells.

To conclude, $Ca_V1.2$-TS channels exhibit greater Ca^{2+} flux, which increases $[Ca^{2+}]$ in both the cytosol and the SR. This Ca^{2+}-overloaded state leads to increases in Ca^{2+} spark frequency and amplitude, AP-evoked $[Ca^{2+}]_i$ transients, and probability of Ca^{2+} waves. The increase in $Ca_V1.2$-TS Ca^{2+} flux also leads to increased SR Ca^{2+} load, thus increasing EC coupling gain. The non-linear relationship between $Ca_V1.2$-TS expression and Ca^{2+} waves shows that even low levels of $Ca_V1.2$-TS can induce dramatic effects on cell Ca^{2+} levels. These conditions combine to create a cell environment prone to arrhythmogenic spontaneous SR Ca^{2+} release.

Supplementary Material

Refer to Web version on PubMed Central for supplementary material.

Acknowledgments

We thank Ms. Jennifer Cabarrus for technical assistance, and Drs. Jose Mercado and Claudia Moreno for editing the manuscript. This study was supported by NIH grant HL085686 and the ARCS Foundation.

References

1. López-López JR, Shacklock PS, Balke CW, Wier WG. Local calcium transients triggered by single L-type calcium channel currents in cardiac cells. Science. 1995; 268:1042–1045. [PubMed: 7754383]
2. Niggli E, Lederer WJ. Voltage-independent calcium release in heart muscle. Science. 1990; 250:565–568. [PubMed: 2173135]

3. Santana LF, Cheng H, Gomez AM, Cannell MB, Lederer WJ. Relation between the sarcolemmal Ca^{2+} current and Ca^{2+} sparks and local control theories for cardiac excitation-contraction coupling. Circ Res. 1996; 78:166–171. [PubMed: 8603501]
4. Cannell MB, Cheng H, Lederer WJ. The control of calcium release in heart muscle. Science. 1995; 268:1045–1049. [PubMed: 7754384]
5. Fabiato A. Calcium-induced release of calcium from the cardiac sarcoplasmic reticulum. Am J Physiol. 1983; 245:C1–C14. [PubMed: 6346892]
6. Cheng H, Lederer WJ, Cannell MB. Calcium sparks: elementary events underlying excitation-contraction coupling in heart muscle. Science. 1993; 262:740–744. [PubMed: 8235594]
7. Splawski I, Timothy KW, Decher N, Kumar P, Sachse FB, Beggs AH, et al. Severe arrhythmia disorder caused by cardiac L-type calcium channel mutations. Proc Natl Acad Sci U S A. 2005; 102:8089–8096. discussion 6-8. [PubMed: 15863612]
8. Hess P, Lansman JB, Tsien RW. Different modes of Ca channel gating behaviour favoured by dihydropyridine Ca agonists and antagonists. Nature. 1984; 311:538–544. [PubMed: 6207437]
9. Erxleben C, Liao Y, Gentile S, Chin D, Gomez-Alegria C, Mori Y, et al. Cyclosporin and Timothy syndrome increase mode 2 gating of CaV1.2 calcium channels through aberrant phosphorylation of S6 helices. Proc Natl Acad Sci U S A. 2006; 103:3932–3927. [PubMed: 16537462]
10. Tsien RW, Bean BP, Hess P, Lansman JB, Nilius B, Nowycky MC. Mechanisms of calcium channel modulation by beta-adrenergic agents and dihydropyridine calcium agonists. J Mol Cell Cardiol. 1986; 18:691–710. [PubMed: 2427730]
11. Barrett CF, Tsien RW. The Timothy syndrome mutation differentially affects voltage- and calcium-dependent inactivation of CaV1.2 L-type calcium channels. Proc Natl Acad Sci U S A. 2008; 105:2157–2162. [PubMed: 18250309]
12. Splawski I, Timothy KW, Sharpe LM, Decher N, Kumar P, Bloise R, et al. Ca(V)1.2 calcium channel dysfunction causes a multisystem disorder including arrhythmia and autism. Cell. 2004; 119:19–31. [PubMed: 15454078]
13. Cheng EP, Yuan C, Navedo MF, Dixon RE, Nieves-Cintron M, Scott JD, et al. Restoration of normal L-type Ca2+ channel function during Timothy syndrome by ablation of an anchoring protein. Circ Res. 2011; 109:255–261. [PubMed: 21700933]
14. Thiel WH, Chen B, Hund TJ, Koval OM, Purohit A, Song LS, et al. Proarrhythmic defects in Timothy syndrome require calmodulin kinase II. Circulation. 2008; 118:2225–2234. [PubMed: 19001023]
15. Yazawa M, Hsueh B, Jia X, Pasca AM, Bernstein JA, Hallmayer J, et al. Using induced pluripotent stem cells to investigate cardiac phenotypes in Timothy syndrome. Nature. 2011; 471:230–234. [PubMed: 21307850]
16. Shioya T. A simple technique for isolating healthy heart cells from mouse models. J Physiol Sci. 2007; 57:327–335. [PubMed: 17980092]
17. Rossow CF, Dilly KW, Santana LF. Differential Calcineurin/NFATc3 Activity Contributes to the I_{to} Transmural Gradient in the Mouse Heart. Circ Res. 2006; 98:1306–1313. [PubMed: 16614306]
18. Grynkiewicz G, Poenie M, Tsien RY. A new generation of Ca^{2+} indicators with greatly improved fluorescence properties. J Biol Chem. 1985; 260:3440–3450. [PubMed: 3838314]
19. Maravall M, Mainen ZF, Sabatini BL, Svoboda K. Estimating intracellular calcium concentrations and buffering without wavelength ratioing. Biophys J. 2000; 78:2655–2667. [PubMed: 10777761]
20. Catterall WA. Structure and regulation of voltage-gated Ca^{2+} channels. Annual review of cell and developmental biology. 2000; 16:521–555.
21. Adachi-Akahane S, Cleemann L, Morad M. Cross-signaling between L-type Ca2+ channels and ryanodine receptors in rat ventricular myocytes. J Gen Physiol. 1996; 108:435–454. [PubMed: 8923268]
22. Yarotskyy V, Gao G, Peterson BZ, Elmslie KS. The Timothy syndrome mutation of cardiac CaV1.2 (L-type) channels: multiple altered gating mechanisms and pharmacological restoration of inactivation. J Physiol. 2009; 587:551–565. [PubMed: 19074970]
23. Oliveria SF, Dell'Acqua ML, Sather WA. AKAP79/150 anchoring of calcineurin controls neuronal L-type Ca^{2+} channel activity and nuclear signaling. Neuron. 2007; 55:261–275. [PubMed: 17640527]

24. Navedo MF, Cheng EP, Yuan C, Votaw S, Molkentin JD, Scott JD, et al. Increased coupled gating of L-type Ca2+ channels during hypertension and Timothy syndrome. Circ Res. 2010; 106:748–756. [PubMed: 20110531]
25. Gold MG, Stengel F, Nygren PJ, Weisbrod CR, Bruce JE, Robinson CV, et al. Architecture and dynamics of an A-kinase anchoring protein 79 (AKAP79) signaling complex. Proc Natl Acad Sci U S A. 2011; 108:6426–6431. [PubMed: 21464287]
26. Bers DM, Bassani JW, Bassani RA. Competition and redistribution among calcium transport systems in rabbit cardiac myocytes. Cardiovascular research. 1993; 27:1772–1777. [PubMed: 8275522]
27. Balke CW, Egan TM, Wier WG. Processes that remove calcium from the cytoplasm during excitation- contraction coupling in intact rat heart cells. J Physiol. 1994; 474:447–462. [PubMed: 8014906]
28. Maier LS, Zhang T, Chen L, DeSantiago J, Brown JH, Bers DM. Transgenic CaMKIIdeltaC overexpression uniquely alters cardiac myocyte Ca2+ handling: reduced SR Ca2+ load and activated SR Ca2+ release. Circ Res. 2003; 92:904–911. [PubMed: 12676813]
29. Guo T, Zhang T, Mestril R, Bers DM. Ca2+/Calmodulin-dependent protein kinase II phosphorylation of ryanodine receptor does affect calcium sparks in mouse ventricular myocytes. Circ Res. 2006; 99:398–406. [PubMed: 16840718]
30. Bradshaw JM, Kubota Y, Meyer T, Schulman H. An ultrasensitive Ca2+/calmodulin-dependent protein kinase II-protein phosphatase 1 switch facilitates specificity in postsynaptic calcium signaling. Proc Natl Acad Sci U S A. 2003; 100:10512–10517. [PubMed: 12928489]
31. Saucerman JJ, Bers DM. Calmodulin mediates differential sensitivity of CaMKII and calcineurin to local Ca2+ in cardiac myocytes. Biophys J. 2008; 95:4597–4612. [PubMed: 18689454]
32. Song Q, Saucerman JJ, Bossuyt J, Bers DM. Differential integration of Ca2+-calmodulin signal in intact ventricular myocytes at low and high affinity Ca2+-calmodulin targets. J Biol Chem. 2008; 283:31531–31540. [PubMed: 18790737]
33. Dixon RE, Yuan C, Cheng EP, Navedo MF, Santana LF. Ca2+ signaling amplification by oligomerization of L-type Cav1.2 channels. Proc Natl Acad Sci U S A. 2012; 109:1749–1754. [PubMed: 22307641]
34. Cheng H, Lederer MR, Lederer WJ, Cannell MB. Calcium sparks and $[Ca^{2+}]_i$ waves in cardiac myocytes. Am J Physiol. 1996; 270:C148–C159. [PubMed: 8772440]

Highlights

- Sarcolemmal Ca2+ “leak” and diastolic [Ca2+]i are higher in TS than in WT cells.
- Sarcoplasmic reticulum Ca2+ load is higher in TS than in WT myocytes.
- Ca2+ release increases the rate of inactivation of CaV1.2 currents in TS myocytes.
- Few CaV1.2---TS are sufficient to induce maximal change in [Ca2+]i.
- Ca2+---overload in TS creates increased arrhythmogenic events.

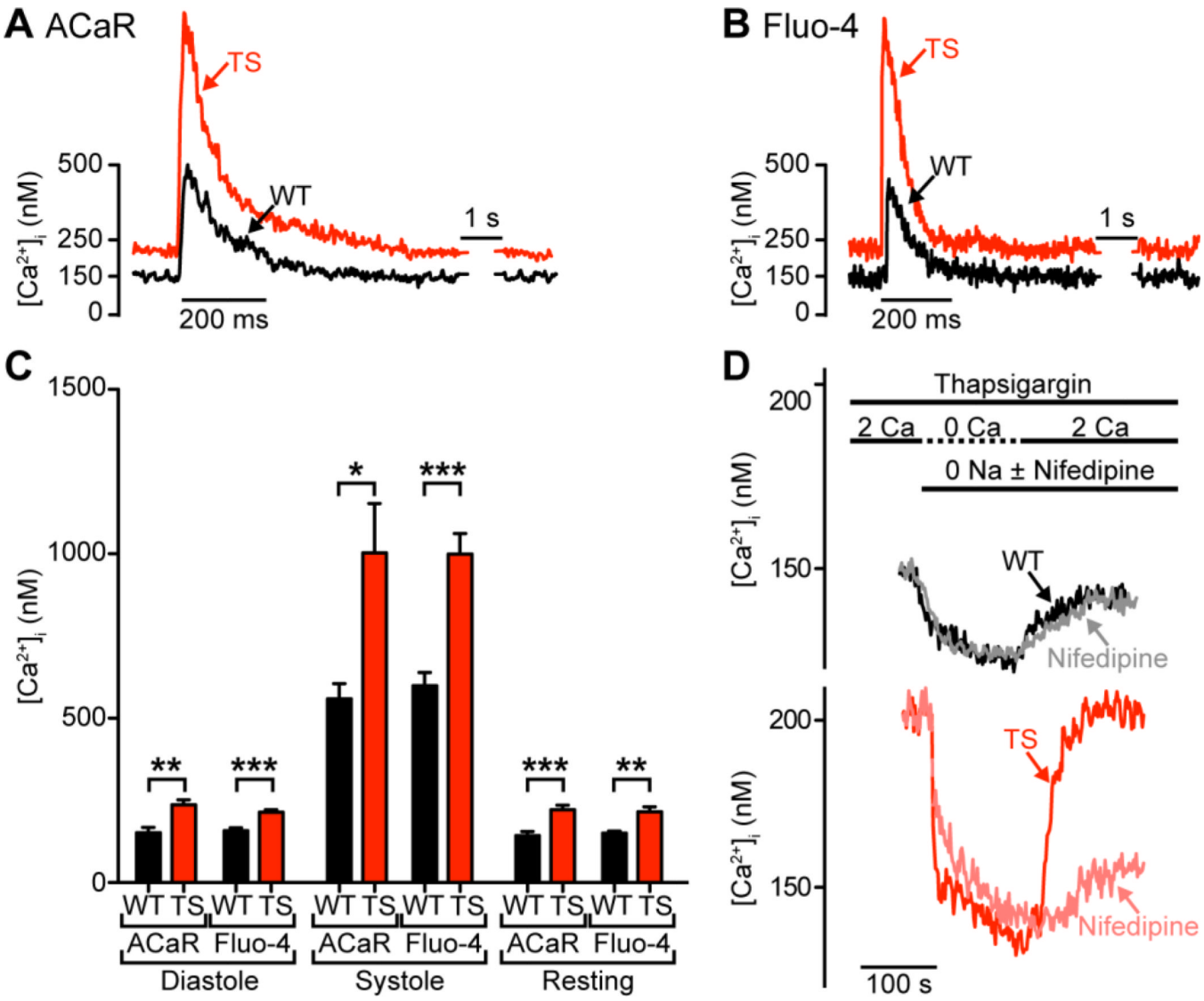

Figure 1. Higher diastolic, systolic, and resting $[Ca^{2+}]_i$ and larger sarcolemmal leak in TS cells

A–B, representative $[Ca^{2+}]_i$ (nM) traces of WT (*black*) and TS (*red*) cells in diastole, systole, and at rest measured using the indicators ACaR (**A**) and Fluo-4 (**B**). **C**, bar plots of the mean ± S.E.M. of the diastolic, systolic, and resting $[Ca^{2+}]_i$ (nM) levels of WT and TS cells measured using each indicator. **D**, representative time courses of WT (*black*) and TS (*red*) cell sarcolemmal $[Ca^{2+}]_i$ (nM) leak (upon application of thapsigargin and removal of Na^+ and Ca^{2+} from bath) and recovery (upon restoration of 2 mM Ca^{2+} to bath). Grey and pink traces indicate same experiment upon application of nifedipine.

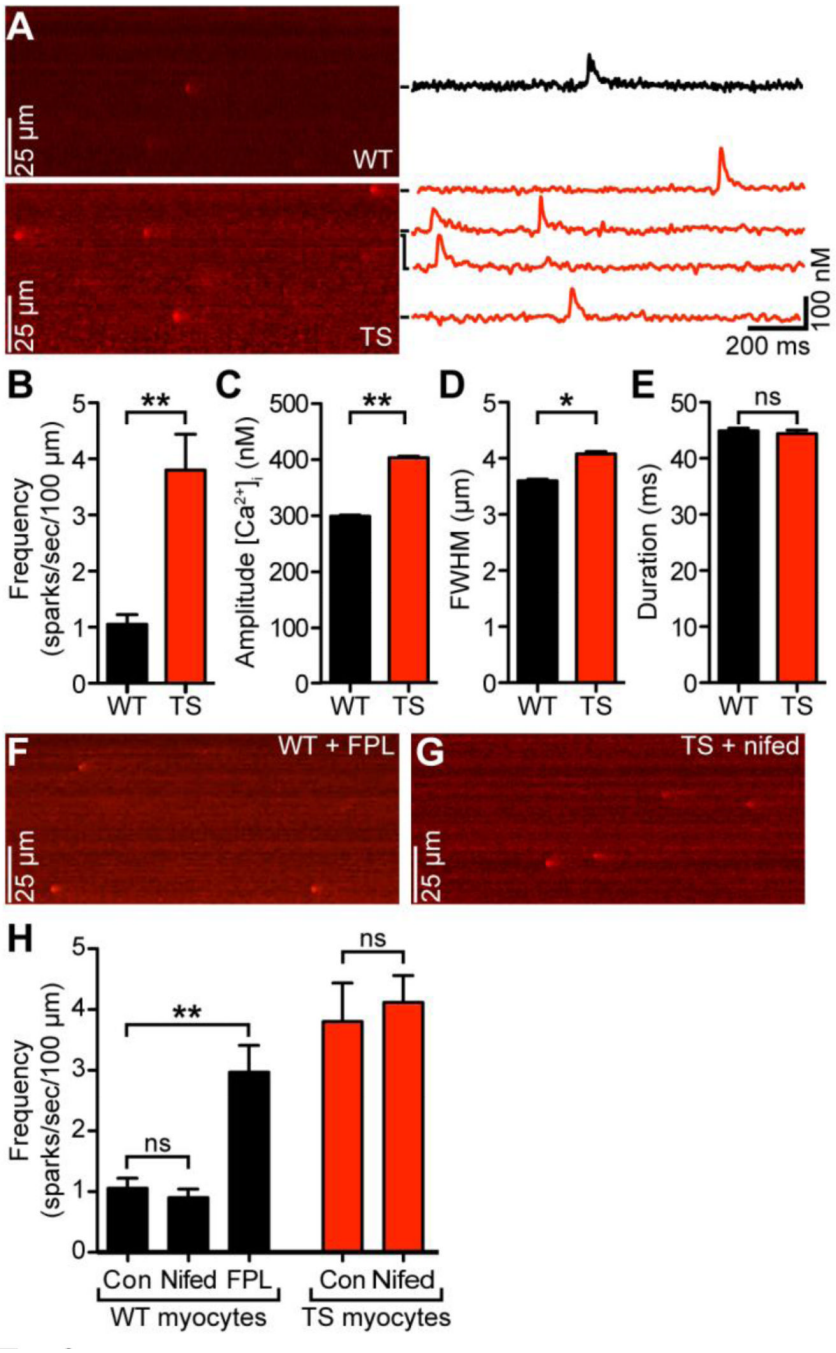

Figure 2. Higher Ca^{2+} spark activity in TS cells

A, representative confocal line-scan images from WT (*above*) and TS (*below*) cells. $[Ca^{2+}]_i$ (nM) plotted to the right for each spark seen, marked by black bars. **B–E**, bar plots of the mean ± S.E.M. of the frequency (**B**), amplitude (**C**), full width at half-maximal amplitude (**D**), and duration (**E**) of Ca^{2+} sparks in WT and TS myocytes. **F**, representative confocal line-scan image of a WT cell upon long-term application of FPL 64176. **G**, representative confocal line-scan image of a TS cell upon short-term application of nifedipine. **H**, bar plots of the mean ± S.E.M. frequency of Ca^{2+} sparks in WT myocytes upon application of FPL 64176 and nifedipine and TS myocytes upon application of nifedipine.

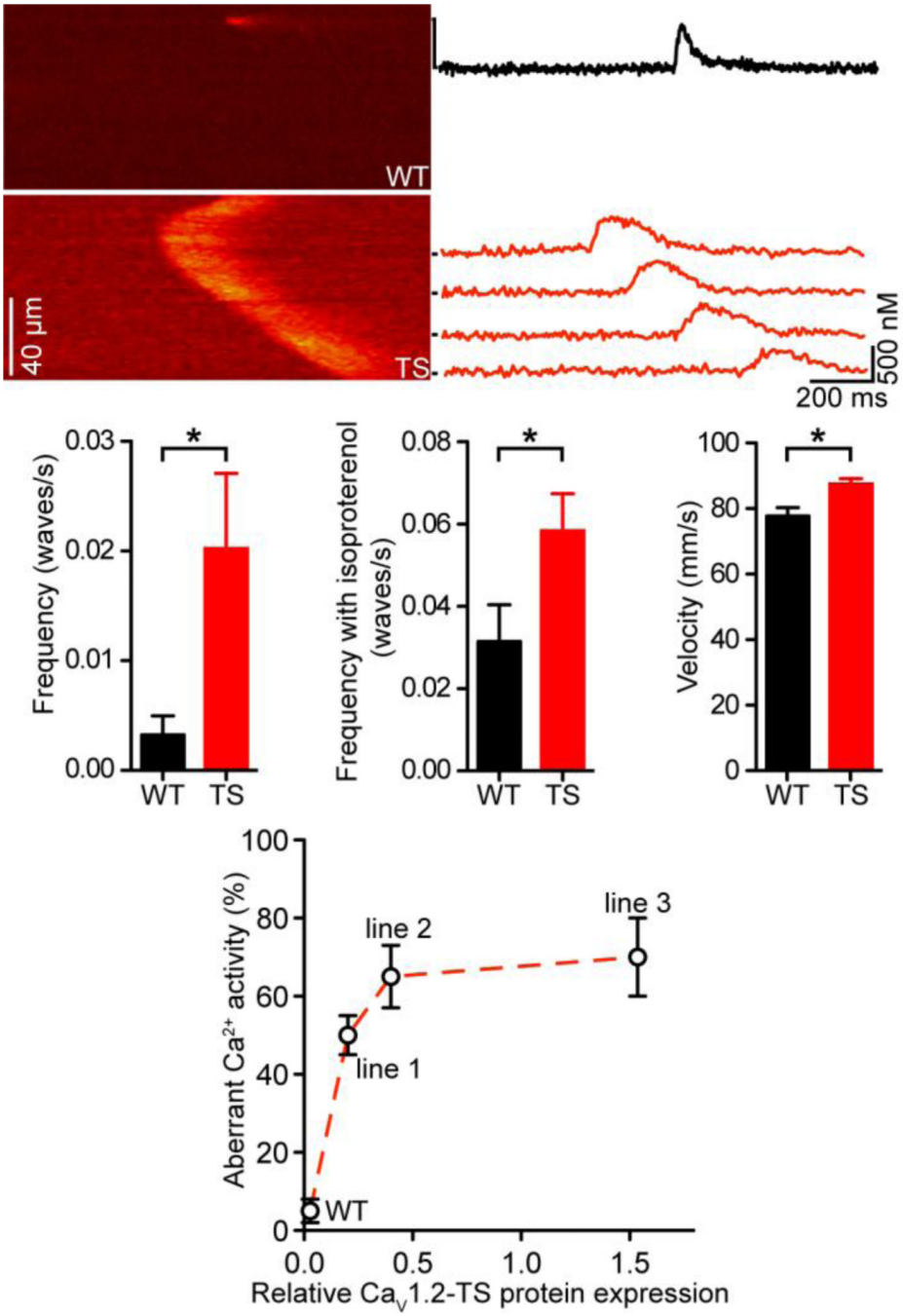

Figure 3. Higher Ca^{2+} wave activity in TS cells

A, representative confocal line-scan images of a large spark in a WT cell (*above*) and a Ca^{2+} wave in a TS cell (*below*). $[Ca^{2+}]_i$ (nM) plotted to the right for each line marked by black bars. **B–D**, bar plots of the mean ± S.E.M. of the frequency (**B**), frequency upon application of 100 nM isoproterenol (**C**), and velocity (**D**) of Ca^{2+} waves in WT and TS myocytes. **E**, plot of relative $Ca_V1.2$-TS expression (x-axis) vs. frequency of aberrant Ca^{2+} activity (%) (y-axis).

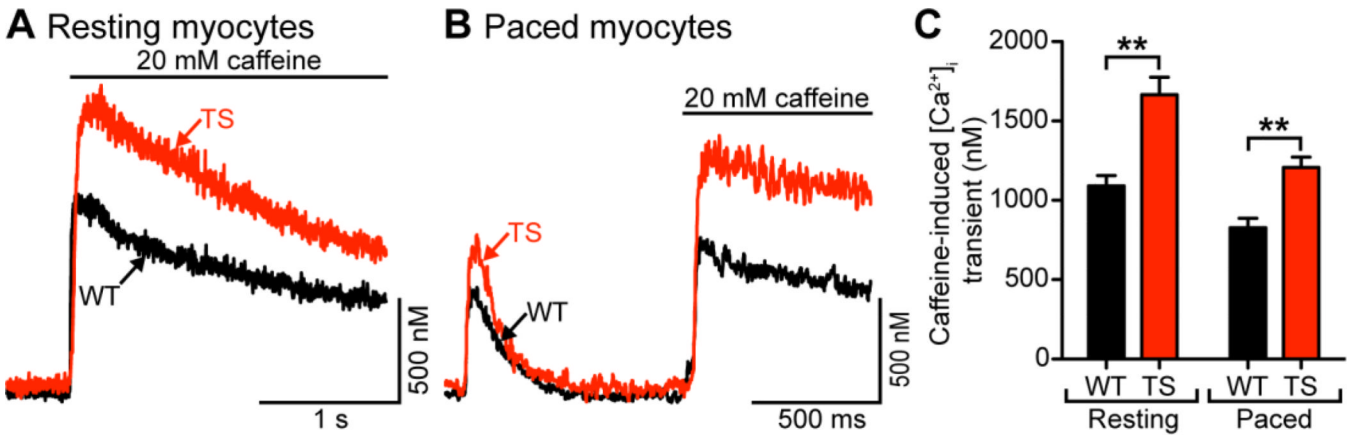

Figure 4. Higher resting and paced SR load in TS cells

A, representative SR Ca^{2+} release upon application of 20 mM caffeine in resting WT (*black*) and TS (*red*) cells. **B**, representative SR Ca^{2+} release upon application of 20 mM caffeine in WT (*black*) and TS (*red*) cells paced at 1 Hz. **C**, bar plot of the mean ± S.E.M. of SR Ca^{2+} release upon application of 20 mM caffeine in resting and paced WT and TS myocytes.

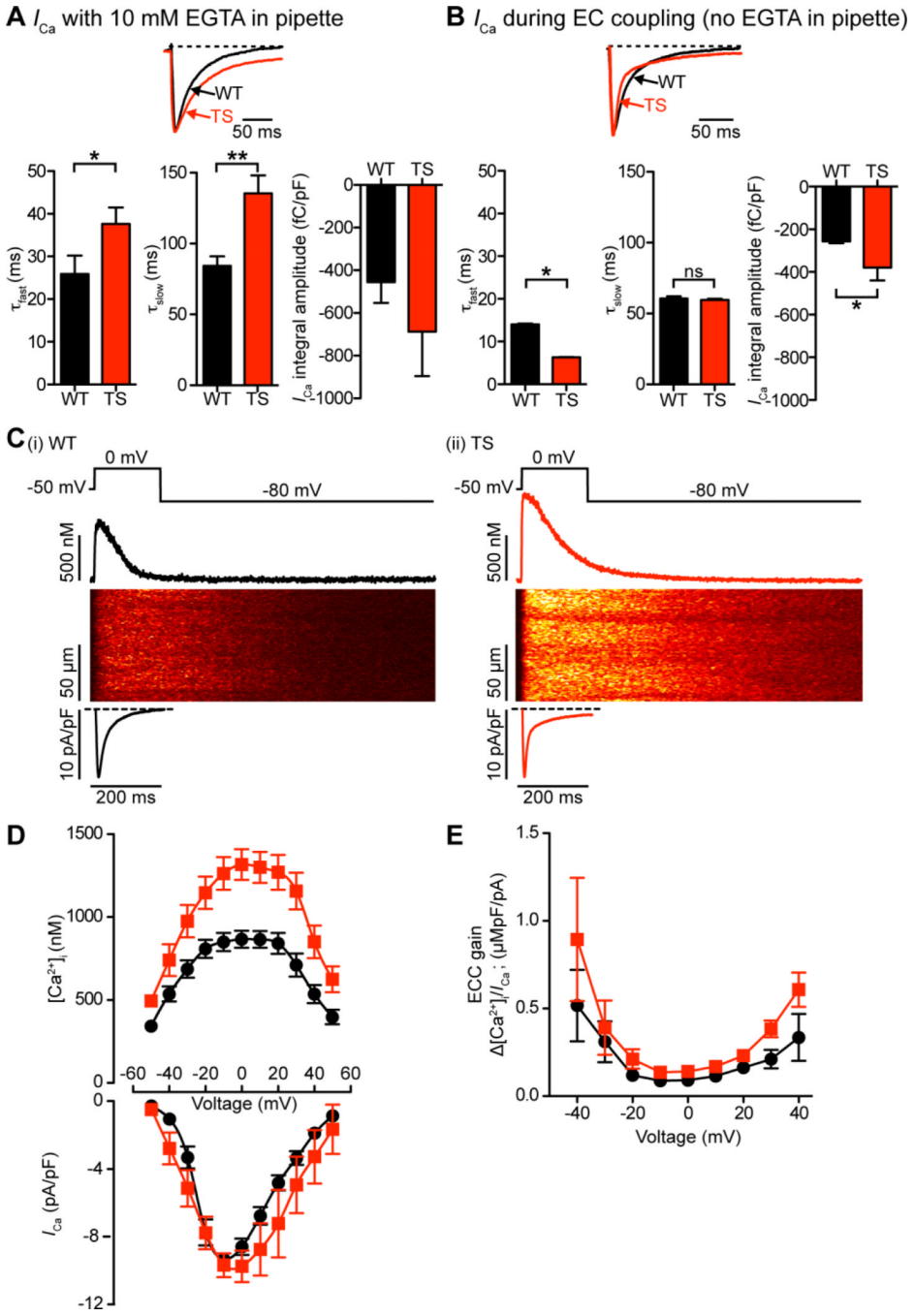

Figure 5. Higher SR Ca^{2+} release during EC coupling in TS cells increases the rate of inactivation of I_{Ca}

A–B, representative I_{Ca} records normalized to peak from TS and WT myocytes dialyzed with an intracellular solution containing (**A**) or lacking (**B**) 10 mM of the Ca^{2+} chelator EGTA. Currents were evoked by a voltage step from −50 mV to 0 mV in the presence of 2 mM external Ca^{2+}. *Below*, bar plots of the mean ± S.E.M. of the inactivation components of I_{Ca}: τ_{fast} (ms), τ_{slow} (ms), and current integral (fC/pF) in WT and TS myocytes. **C**, representative I_{Ca} and confocal line-scan images from WT (i) and TS (ii) cells. I_{Ca} and $[Ca^{2+}]_i$ transients were evoked by a 200 ms voltage step from −50 to 0 mV. Traces showing the time course of I_{Ca} and $[Ca^{2+}]_i$ in these cells are shown below and above the line-scan

images, respectively. **D**, voltage dependence of the amplitude of the $[Ca^{2+}]_i$ transient on positive y-axis, current-voltage relationship of I_{Ca} on negative y-axis, for both WT (*black*) and TS (*red*) cells. **E**, voltage dependence of EC coupling (ECC) gain for WT (*black*) and TS (*red*).

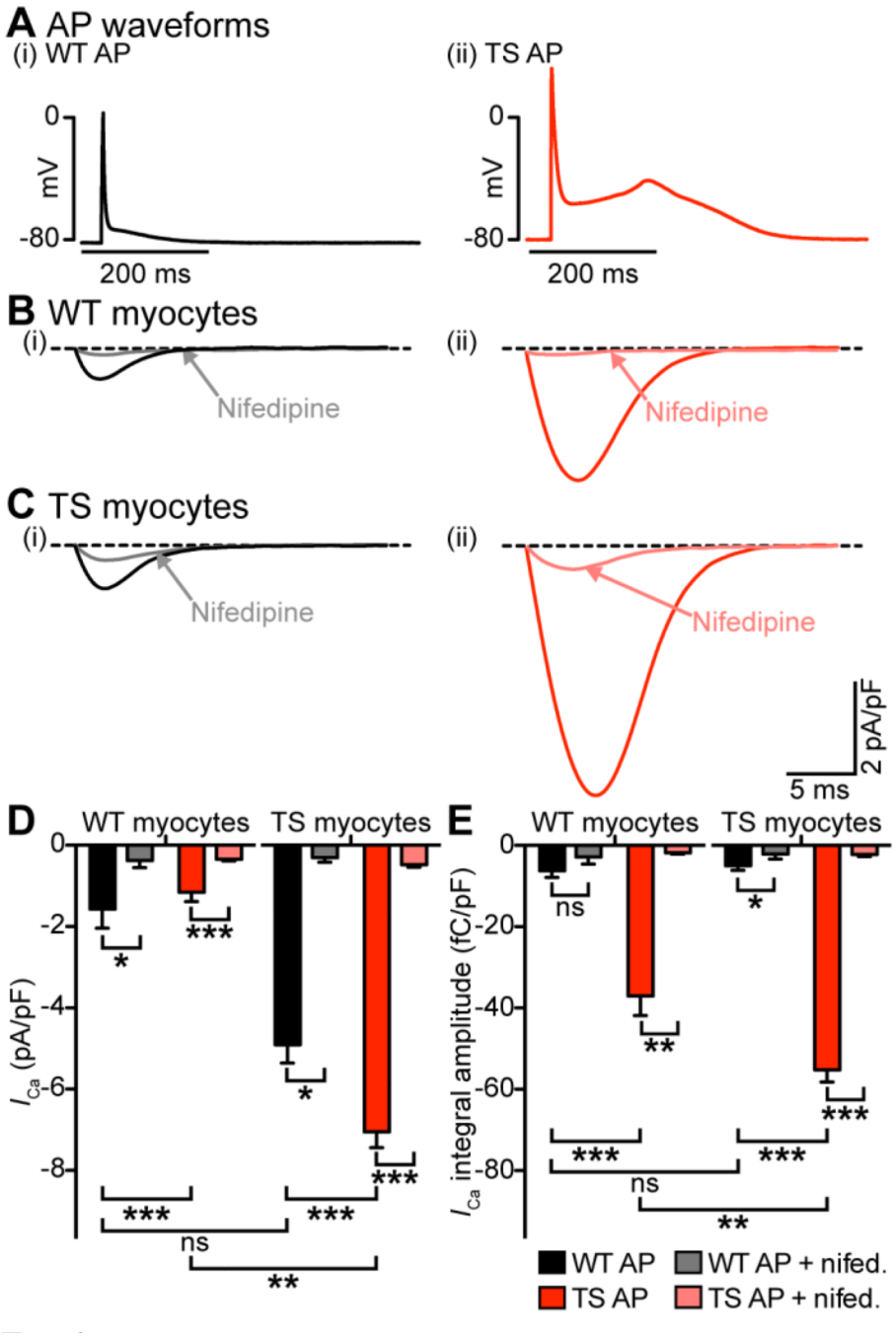

Figure 6. Differences in AP waveform contributes to differences in L-type Ca^{2+} current between WT and TS myocytes

A, representative WT (i) and TS (ii) APs. **B–C** Current traces from a representative WT myocyte (**B**) and a TS myocyte (**C**) stimulated with the WT AP (i) or TS AP (ii). Traces recorded in the presence of 10 μM nifedipine are labeled and indicated with arrows. **D–E**, bar plots of the mean ± S.E.M. of the amplitude of I_{Ca} (**D**) and the current integral (**E**) in WT and TS myocytes stimulated with the WT or TS APs with and without 10 μM nifedipine.

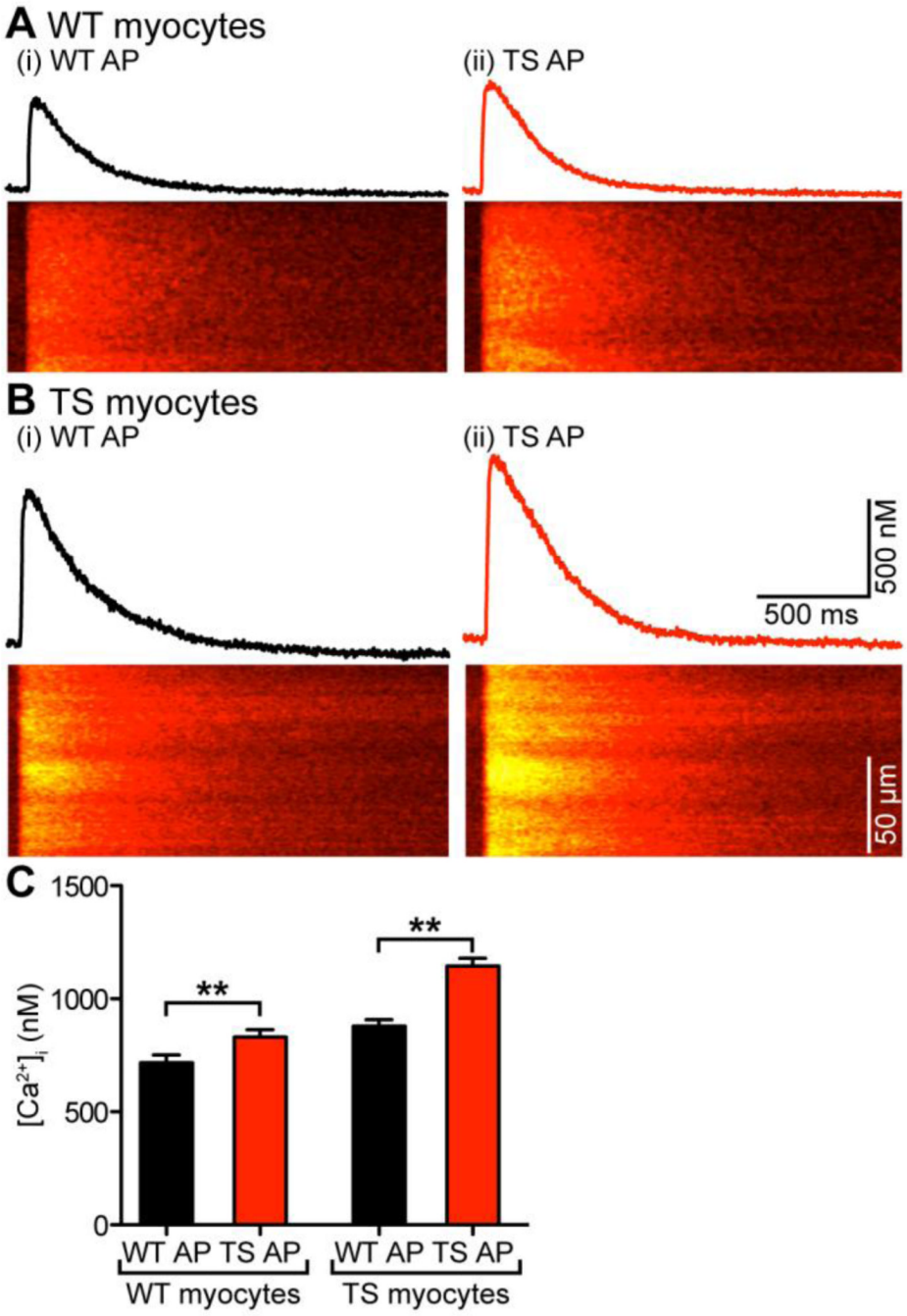

Figure 7. Differences in AP waveform contributes to differences in $[Ca^{2+}]_i$ between WT and TS myocytes

A–B, $[Ca^{2+}]_i$ transients and confocal line-scan images from a representative WT (**A**) and TS myocyte (**B**) stimulated with the WT AP (i) or TS AP (ii). **C**, bar plot of the mean ± S.E.M. of the amplitude of the $[Ca^{2+}]_i$ transient in WT and TS myocytes stimulated with the WT or TS APs.